Particle & Particle Systems Characterization

Particle & Particle Systems Characterization
www.particle-journal.com

RESEARCH ARTICLE OPEN ACCESS

Removal of Inorganic Contaminants Using Sodalite Synthesized From Alum Sludge

Raquel Cardoso Machado[1] | Vinicius Ferraz Majaron[1,2] | Alexandre Antonio Fidelis Martins Junior[1,3] | Nathália Liz Barrios[1,3] | Welton de Araujo Cintra Junior[4,5] | Ricardo Bortoletto-Santos[1,4] | Caue Ribeiro[1]

[1]Nanotechnology National Laboratory For Agriculture (LNNA), Embrapa Instrumentation, São Carlos, São Paulo, Brazil | [2]São Carlos Institute of Chemistry (IQSC), University of São Paulo (USP), São Carlos, São Paulo, Brazil | [3]Federal University of São Carlos (UFSCar), São Carlos, São Paulo, Brazil | [4]Postgraduate Program in Environmental Technology, University of Ribeirão Preto (UNAERP), Ribeirão Preto, São Paulo, Brazil | [5]Sanitation Company of the State of São Paulo (SABESP), Franca, São Paulo, Brazil

Correspondence: Caue Ribeiro (caue.ribeiro@embrapa.br)

Received: 9 December 2025 | **Revised:** 19 April 2026 | **Accepted:** 24 April 2026

Keywords: adsorption | alum sludge | hydrothermal treatment | metals | sodalite

ABSTRACT

The growing concern over water contamination by potentially toxic metals underscores the need for sustainable and cost-effective remediation strategies. In this study, sodalite (SOD-Na) was synthesized from alum sludge (AS), a by-product of water treatment plants rich in Si and Al, through a hydrothermal process in an autoclave. Zeolitic concentrate was characterized by x-ray diffraction (XRD), scanning electron microscopy (SEM), x-ray fluorescence (XRF), Brunauer Emmet Teller (BET) method, and zeta potential analysis, confirming the formation of sodalite with mesoporous structure and surface charge favorable to cation adsorption. Adsorption experiments demonstrated high affinity for Pb^{2+} (189 mg g^{-1}), Cd^{2+} (121 mg g^{-1}), and Ni^{2+} (58.4 mg g^{-1}), whereas limited adsorption was observed for Cr^{6+} ($Cr_2O_7^{2-}$) (8.2 mg g^{-1}), consistent with the material's negative surface charge and ion-exchange mechanism. Tests with real wastewater confirmed the material's applicability, showing Ni^{2+} removal capacity of 26.5 mg g^{-1} despite competitive interactions with coexisting ions. These findings highlight the potential of sodalite synthesized from alum sludge as an effective and sustainable adsorbent for wastewater treatment, contributing to circular economy strategies and reducing environmental liabilities.

1 | Introduction

Growing concern for the environment has driven the search for sustainable solutions, especially in treating emerging contaminants, such as potentially toxic metals, which compromise public health and ecological balance. Moreover, the inadequate disposal of urban and industrial waste worsens water pollution, with more than 80% of the world's sewage being discharged without treatment, increasing the risk of kidney, neurological, and cancer diseases [1–6]. Among potentially toxic metals frequently detected in industrial and urban effluents, Pb^{2+}, Cd^{2+}, Ni^{2+}, and Cr^{6+} are of particular environmental concern due to their high toxicity, persistence, and widespread occurrence in wastewater streams. Lead and cadmium are associated with severe neurological, renal, and carcinogenic effects even at low concentrations, as well as nickel becomes toxic at elevated levels and is commonly found in electroplating, metallurgical, and mining effluents. In addition, chromium, especially in its hexavalent form, is highly mobile, carcinogenic, and frequently released from tanning, pigment, and metal-finishing industries. In view of this, efforts are needed to improve waste purification and recovery techniques, and for that, different materials have been used to remove contaminant ions from waste, such as sustainable carbon material and zeolites from sludge produced

in water treatment plants, promoting the circular economy, and contributing to the UN Sustainable Development Goals [7–12].

In this scenario, waste valorization emerges as an alternative for producing materials that can be reused within the circular chain at low cost. Thus, the production of zeolites from sludge generated by water treatment plants has the potential to remove contaminants, such as potentially toxic metals, while also recovering nutrients of interest to industry and agriculture [13, 14]. However, any synthesis route involving waste materials must consider process cost and sustainability constraints. Therefore, it is essential to operate under mild hydrothermal conditions, low temperature and short reaction time, while minimizing compositional variations and the addition of external raw materials.

Sodalite ($Na_8[Al_6Si_6O_{24}]Cl_2$) is a zeolitic material that stands out for its ion exchange capacity and ion selectivity and is capable of interacting with charged metals due to the presence of anionic ions in its channels. Moreover, the synthesis can be carried out from natural sources or industrial waste containing significant levels of Si and Al, such as WTP sludge, which is rich in Si and Al [15, 16]. Cationic exchange capacity (CEC) is one of the most important features of zeolitic materials because it is related to the adsorption capacity of different substances, such as gases and metal ions [17]. Studies indicate that sodalite is a sustainable alternative for treating effluent water, being effective in the adsorption of emerging substances such as pharmaceuticals and microplastics, as well as ammonium, organic products, and potentially toxic metals, i.e., lead, cadmium, and nickel, among others [18–20].

The use of sodalite synthesized from waste, such as WTP sludge, is directly linked to the circular economy, developing environmental liabilities into high-value-added materials. This approach reduces waste disposal and minimizes environmental impacts, promoting sustainability by aligning recycling and impact reduction with the Sustainable Development Goals (SDGs) [12, 21, 22]. Thus, the present study proposes the synthesis of a mineral concentrate containing sodalite from WTP sludge and uses the low-cost hydrothermal method in mild conditions to evaluate its effectiveness as an adsorbent for removing potentially toxic metals from aqueous media and real effluents. The selection of Pb^{2+}, Cd^{2+}, Ni^{2+}, and Cr^{6+} allow evaluating the adsorption selectivity of zeolitic materials toward divalent cations in contrast to anionic species ($Cr_2O_7^{2-}$), providing insights into the role of surface charge, ion-exchange capacity, and electrostatic interactions in the adsorption mechanism. Moreover, it is worth noting that for environmental applications, such as contaminant adsorption, high phase purity is not required. Zeolitic concentrates composed predominantly of sodalite are sufficient to ensure effective performance, providing a more economical and sustainable alternative to conventional high-purity zeolites. The analysis of adsorption profiles and performance under different experimental conditions provided essential information to validate the use of this material as a sustainable, effective solution for effluent treatment.

Although zeolite synthesis from alum sludge has been previously reported, most studies focus on maximizing crystallinity or developing modified materials under energy-intensive conditions. In contrast, the present work emphasizes process simplicity, mild hydrothermal conditions, and the production of a functional zeolitic concentrate suitable for environmental remediation. The integration of waste valorization, realistic wastewater assessment, and comparative adsorption behavior under multi-ion competition distinguishes this study from previous approaches.

2 | Materials and Methods

2.1 | Synthesis of Zeolitic Concentrate

Alum sludge (AS) was acquired from a water treatment plant in Hortolândia (São Paulo, Brazil), in which aluminum polychloride serves as a coagulant for water treatment. The material was collected and dried at 40°C in an oven for four days, as well as ground in a ball mill (Marconi, Brazil) and sieved to a size of <0.5 mm.

The synthesis process was adapted from Machado et al. [14]. Alkaline solution (4 mol L^{-1}) was prepared using NaOH (Synth, Brazil), followed by dissolving sodium silicate (Na_2O_3Si; Exodo, Brazil), which is an additional Si source and AS as Si and Al source, considering a Si/Al ratio of 1.7. The mixture was under agitation at 500 rpm for 30 min at 25°C. The homogeneous reaction mixture was transferred to a glass bottle and placed into an autoclave, where the zeolitic concentrate crystallized under static conditions and hydrothermal treatment for 5 h at approximately 1.2 kgf cm^{-3} (equivalent to approximately 120°C). The synthesized material was washed with deionized water until the pH reached eight and then dried in an oven overnight at 100°C (details of the synthesis process are shown in Figure 1).

2.2 | Materials Characterization

The zeolitic concentrate was characterized by x-ray diffraction (XRD, Shimadzu 6000, Japan) with Cu Kα radiation (λ = 1.54178 Å), scan speed of 2° min^{-1}, and in a range 2θ of 4° to 60°, as well as the x-ray Fluorescence (XRF, Malvern Panalytical mini-PaI4, United Kingdom) was used for obtaining mineralogical and chemical composition of the material. Alum sludge was analyzed by inductively coupled plasma optical emission spectrometry (ICP OES, 5110, Agilent Technologies, Mulgrave, Australia) to verify the presence of contaminant elements in its composition.

Scanning Electron Microscopy (SEM) was used to analyze the morphology of the zeolitic concentrate after the sample had been coated with gold in an ionization chamber (BalTec Med. 020, Switzerland), using a microscope equipped with a secondary electron detector (JEOL JSM6510, Japan). Energy dispersive x-ray (EDX) analysis was performed using Thermo Scientific 6742A coupled to a SEM. The samples were coated with carbon in an ionization chamber (SCD050/LEICA). The acquisition parameters were 15 kV, a working distance of 10 mm, and 100 scans.

The external surface area of zeolitic materials was determined according to the Brunauer–Emmett–Teller (BET) method from the N_2 adsorption–desorption isotherms using an ASAP (Micromeritics Corporation 2020, United States America), and the size distribution of the zeolitic concentrate was analyzed with Zetasizer Advance equipment (Malvern Panalytical, United

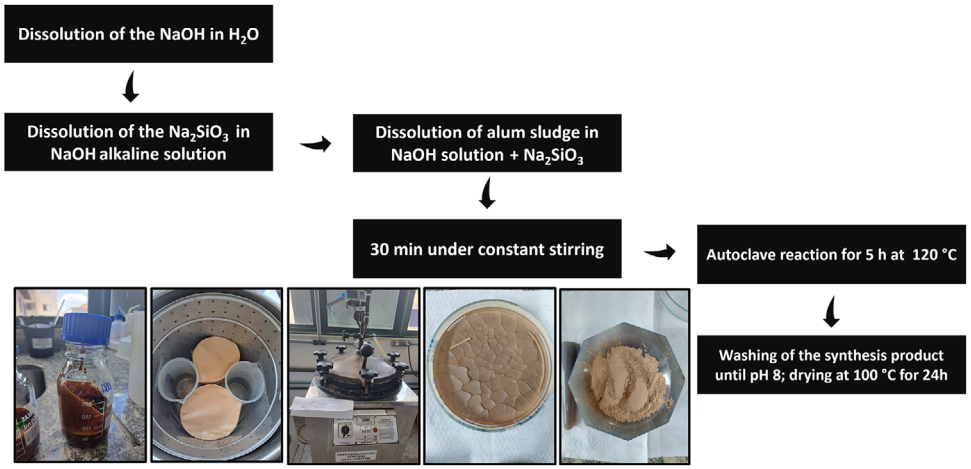

FIGURE 1 | Scheme of the synthesis process for obtaining zeolitic concentrate from alum sludge.

Kingdom). Moreover, the determination of the residual surface charge was obtained at different pH levels using the Zetasizer Advance Series equipment from Malvern Instruments, Ultra model (Red Label). Two milligrams of zeolite synthesized from alum sludge were added to a beaker containing 20 mL of Milli-Q water. The system was dispersed in an Ultrasonic Sonicator (Branson S-450D), using a 90 s cycle, 30% amplitude, and a 3/16-inch (5 mm) diameter tapered tip microtip. The pH value was monitored using a Gehaka pH meter (model PG2000). Hydrochloric acid (0.025 M) and sodium hydroxide (0.025 M) were used to adjust the pH to 2, 5, 7, and 9.

2.3 | Adsorption Experiments Using Zeolite Concentrates

Approximately 50 mg of zeolitic concentrate was added to 50 mL of a solution containing Cr^{6+} and Ni^{2+} at 250, 500, and 1000 mg L^{-1}, as well as Cd^{2+} and Pb^{2+} at 250, 500, 1000, 1500, and 2000 mg L^{-1}. The solutions containing the analytes were prepared by dissolving salts, such as lead chloride ($PbCl_2$), nickel chloride ($NiCl_2$), cadmium nitrate ($Cd(NO_3)_2$), and potassium dichromate ($K_2Cr_2O_7$), in deionized water. The mixture was kept under orbital agitation at 150 rpm, at 25°C for 48 h. The contact time of 48 h was selected to ensure that the adsorption equilibrium was reached for all evaluated systems. This conservative duration accounts for possible intraparticle diffusion effects typically observed in zeolitic materials and avoids underestimation of maximum adsorption capacities. The low experimental deviations and the stabilization of adsorption capacity and final pH values across different initial concentrations indicate that equilibrium conditions were achieved within this timeframe.

The solutions were analyzed for flame atomic absorption spectrometry (FAAS, Perkin Elmer, PinAAcle 900T, USA), using a flame composed of synthetic air/acetylene (10 mL/2.5 mL) in the following wavelengths: 228.80, 357.87, 232.00, and 283.31 nm for Cd, Cr, Ni, and Pb, respectively. All adsorption experiments were performed in quadruplicate. For all solutions, both before and after the adsorption experiments, the pH values of each solution were monitored.

The potential of zeolitic concentrate as an adsorbent for the removal of contaminant elements was evaluated using wastewater effluent (real sample) collected from a wastewater treatment plant located in Franca (São Paulo State, Brazil). FAAS performed elemental determination in the effluent after appropriate dilution. The adsorption experiment with the real sample was conducted using the previously described methodology, with 50 mL of wastewater effluent and 50 mg of zeolitic concentrate. It is worth noting that, after the adsorption process, the zeolites were analyzed by energy-dispersive x-ray (EDX) spectroscopy to identify the main adsorbates.

3 | Results and Discussion

3.1 | Mineral and Morphological Composition, Particle Size, and Surface Area of Zeolitic Concentrate Synthesized From Alum Sludge

Figure 2a shows well-defined XRD patterns for sodalite (SOD-Na) and some quartz phases after the crystallization process using an autoclave and 4 mol L^{-1} NaOH. It is possible to observe that the quartz, kaolinite, and $Al(OH)_3$ mineral phases in the alum sludge were considerably reduced during the reaction, indicating that the crystallization process was efficient in converting AS into a zeolitic concentrate, containing SOD-Na phases and impurities as quartz (around 13% SiO_2; the sodalite fraction estimated is 87%). It should be noted that the objective of this study was not the production of highly pure zeolite, but the development of a zeolitic concentrate with sufficient crystallinity and functionality for environmental remediation purposes. For such applications, the presence of minor amorphous or residual mineral phases does not compromise adsorption efficiency.

In the compositional analysis of the alum sludge (Table 1), it was observed that the contaminant element concentrations, such as As, Cd, Cr, and Pb were below the limit of quantification, indicating that the material doesn't represent a risk of leaching from the synthesized SOD-Na. Table 1 also presents the chemical composition of the zeolitic concentrate analyzed by XRF.

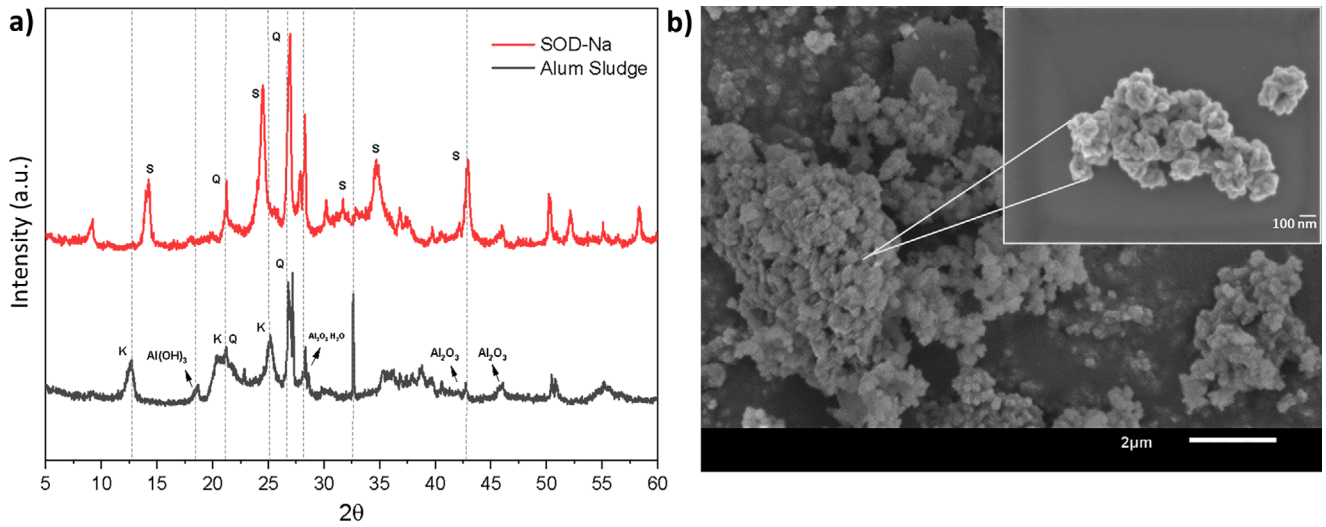

FIGURE 2 | (a) XRD patterns, where S = sodalite, Q = quartz, K = kaolinite and (b) SEM images for SOD-Na synthesized from AS in alkaline medium and autoclave.

TABLE 1 | Determination of elemental concentration in alum sludge analyzed by ICP OES, and oxide concentration determined in the zeolitic concentrate by XRF.

Alum sludge[a)]		SOD-Na[b)]	
Element	**Concentration (%)**	**Oxide**	**Concentration (%)**
Al	10.5 ± 0.09	Al_2O_3	14.474
As	<LOQ	CaO	0.646
Ca	0.20 ± 0.08	Cl	0.052
Cd	<LOQ	F_2O_3	5.995
Cr	<LOQ	K_2O	0.848
Cu	0.02 ± 0.0002	MnO	0.104
Fe	4.16 ± 0.05	P_2O_5	0.434
K	0.25 ± 0.002	SiO_2	30.110
Mg	0.26 ± 0.004	SO_3	0.590
Mn	0.12 ± 0.002	TiO_2	0.713
Na	0.03 ± 0.007	MnO	0.104
Ni	<LOQ	—	—
P	0.35 ± 0.01	—	—
Pb	<LOQ	—	—
S	0.19 ± 0.008	—	—
Zn	<LOQ	—	—

LOQ—limit of quantification of the analysis method.
[a]ICP OES analysis
[b]XRF analysis

The morphology of the zeolitic concentrate is presented in Figure 2b. It is possible to observe smaller and uniform particles, as well as non-uniform aggregate particles, in spherical shapes of varying sizes (SEM images). More details on the material's morphology were obtained using SEM, which revealed smaller spheres, uniform round particles, and aggregates, consistent with the sodalite morphology previously reported in the literature [23–25]. Moreover, the SOD-Na synthesized particles had a particle size of approximately 200 nm, which is lower than that reported by Machado et al. [14]. This difference can be attributed to the crystal formation process, including seeding, alkalinity, temperature, time, and hydrothermal conditions. On the other hand, the

TABLE 2 | Maximum adsorption for Cd^{2+}, Ni^{2+}, Pb^{2+}, and Cr^{6+} using zeolitic concentrate obtained from alum sludge.

Ions adsorbed	mg ion g^{-1} zeolite	mol	Initial pH	Final pH
Pb^{2+}	189 ± 1	1.09	4.68	7.85
Cd^{2+}	121 ± 2	0.93	5.33	6.64
Ni^{2+}	58.4 ± 0.5	1	5.55	6.81
$Cr_2O_7^{2-}$	8.20 ± 0.4	—	4.13	6.65

observed morphology is consistent with sodalite-type aggregates reported in the literature, confirming successful crystallization under mild hydrothermal conditions.

The surface area for zeolitic concentrate determined by the BET method was 32 m^2 g^{-1}, in agreement with the area obtained by Yoldi et al. [26]. Although the surface area obtained for SOD-Na synthesized in this study is similar to zeolites prepared using a hydrothermal reactor, it is worth highlighting that the material synthesized in this study was prepared using a commercial autoclave used for glassware sterilization, i.e., a robust, simple, scalable, and efficient process. According to these authors, differences in surface area and other properties of the synthesized zeolite are related to the synthesis conditions, including the Si/Al ratio, pH, and crystallization time. Moreover, the N_2 adsorption-desorption isotherm shows a hysteresis loop H3 and was classified as Type IV, typical of mesoporous and adsorbent materials [25]. It is important to emphasize that adsorption in zeolitic materials is predominantly governed by framework charge density and cation-exchange capacity rather than solely by external surface area. Therefore, moderate BET values do not necessarily limit adsorption performance.

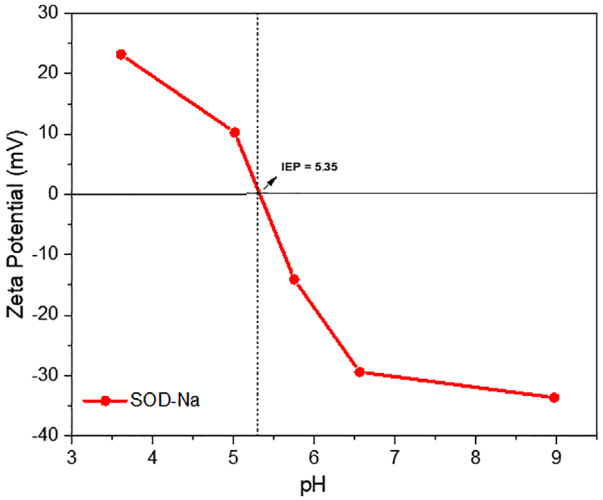

FIGURE 3 | Zeta potential of SOD-Na obtained at different pH values.

3.2 | Contaminant Adsorption From Zeolitic Concentrate

The maximum adsorptions capacities of SOD-Na for Cd^{2+}, Cr^{6+}, Ni^{2+}, and Pb^{2+} were determined and reported in Table 2. The highest adsorption was observed for Pb^{2+} (189 mg g^{-1}), Cd^{2+} (121 mg g^{-1}), and Ni^{2+} (58.4 mg g^{-1}). A similar tendency for ion adsorption was observed for natural zeolites such as clinoptilolite and heulandite, which showed higher affinity for these contaminant ions and the same selectivity (Pb^{2+} > Cd^{2+} > Ni^{2+}) [27]. The maximum adsorption values for Cd^{2+} and Pb^{2+} using SOD-Na as an adsorbent were higher than those found for natural zeolite, ranging from 56 to 92 mg g^{-1} and 123 to 138 mg g^{-1} for Cd^{2+} and Pb^{2+}, according to Dehmani et al. [28]. Moreover, the adsorption value obtained from SOD-Na for Ni (58.4 mg g^{-1}) was higher than those mentioned by Pahlavanzadeh and Motamedi [29], using modified and 3A zeolites (16 and 25 mg g^{-1}, respectively). It is important to note that although higher adsorption capacities have been reported for modified zeolites and nanocomposite materials, such systems frequently require additional chemical functionalization or energy-intensive synthesis steps. The SOD-Na presented in this study emphasizes a simplified and scalable synthesis route, producing a functional zeolitic concentrate directly from alum sludge without post-treatment. From a practical perspective, the balance between adsorption performance, process simplicity, and environmental sustainability represents a key advantage of this approach.

In contrast, the adsorption value for Cr was 8.2 mg g^{-1}, which was significantly lower than the values obtained for the other ions, suggesting that the zeolitic material was not effective at adsorbing Cr^{6+} ions. It is important to mention that Cd, Ni, and Pb were in the solutions as Cd^{2+}, Ni^{2+}, and Pb^{2+} ions (cations), while Cr^{6+} was present as $Cr_2O_7^{2-}$, an anion. This behavior can be explained by analyzing the zeta potential of the SOD-Na, shown in Figure 3. Based on the zeta potential analysis, the synthesized zeolite exhibits an isoelectric point (IEP) at pH 5.35, where the surface charge is neutral. Above this pH, the material carries a negative residual charge, enhancing its affinity for cations. In this context, the adsorbent material remains negatively charged under all conditions, as the final pH values were above the IEP, influencing the interaction between the zeolite and Cr^{6+} in its anionic form.

In this context, the adsorbent material remains negatively charged under all conditions, as the final pH values were above the IEP, influencing the interaction between the zeolite and Cr^{6+} in its anionic form. Beyond surface charge considerations, the adsorption behavior can also be interpreted considering the structural characteristics of sodalite. The aluminosilicate framework contains tetrahedrally coordinated AlO_4 units that generate a permanent negative charge, compensated by exchangeable Na^+ cations located within β-cages. These cages are interconnected through six-membered ring openings that regulate ion

accessibility. Divalent cations can replace exchangeable Na^+ through ion-exchange processes driven by electrostatic interactions and framework charge density. Differences in adsorption performance among Pb^{2+}, Cd^{2+}, and Ni^{2+} may also be influenced by ionic radius, hydration energy, and diffusion constraints within the microporous structure. Thus, adsorption is governed by a combination of framework charge, ion-exchange capacity, electrostatic interactions, and structural accessibility rather than by surface area alone.

Ion-exchange mechanisms drive the majority of adsorption processes using zeolites, as these materials contain exchangeable cations, such as Na^+, K^+, and Ca^{2+}, which facilitate exchange with other cations, such as Cd^{2+}, Ni^{2+}, and Pb^{2+}. According to Velarde et al. [27], this mechanism is influenced by pH and affects cation adsorption, as previously mentioned (Figure 3). Moreover, the surface charge is negative at pH values below eight (the pH of the medium in which the experiments were conducted), allowing Cd^{2+}, Ni^{2+}, and Pb^{2+} cations to be effectively adsorbed via ion exchange and physical adsorption. In contrast, Cr^{6+}, present in the solution as the $Cr_2O_7^{2-}$ anion, exhibits weak interaction with the material's surface, resulting in low adsorption.

Another important aspect to consider is the adsorption of molar ions. The previously observed selectivity for cation adsorption ($Pb^{2+} > Cd^{2+} > Ni^{2+}$) is a common trend in zeolitic materials, as larger ions with lower hydration energy are more easily adsorbed. However, when analyzing the number of moles exchanged rather than the mass (Table 2), it becomes evident that the molar content of ions removed from the solution is nearly the same. These findings suggest that the adsorption behavior of the zeolitic concentrate is strongly selective toward divalent cations. Although ions of varying sizes can access exchange sites, the adsorption process is mainly controlled by ionic valence and hydration energy, favoring cations such as Pb^{2+}, Cd^{2+}, and Ni^{2+} over monovalent or anionic species.

Nickel was selected for evaluation in real wastewater due to its significant concentration in the effluent matrix and its environmental relevance in industrial discharges. Moreover, its intermediate adsorption capacity observed in synthetic systems allows a more representative assessment of competitive adsorption effects under complex ionic conditions. The adsorption capacity of Ni^{2+} from wastewater effluent using the zeolitic concentrate was 26.5 mg g^{-1}, which is about half the value obtained with solutions containing only the individual contaminant ion. The reduction in adsorption capacity compared to single-ion systems reflects the influence of multi-ion competition and increased ionic strength, highlighting the importance of evaluating adsorbents under realistic environmental matrices. When the concentration ratio of competing ions to contaminant ions approaches 20, a trend toward reduced adsorption capacity is observed, particularly in the presence of Ca^{2+}, Mg^{2+}, K^+, Na^+, and Fe^{3+} in this order. Although Fe^{3+} exerts less influence than the other ions, the ratio of 18 for Fe suggests that it may still affect adsorption in a complex matrix, such as wastewater [30].

Considering the concentrations presented in Table 3, a general reduction in several elements (Fe, Cd, Pb, Zn, and Ca) after adsorption indicates that the zeolitic concentrate synthesized from alum sludge acts as a broad-spectrum adsorbent, capable

TABLE 3 | Elemental concentration (mg L^{-1}) in wastewater determined by FAAS.

Elements	Ca	Cd	Cr	Cu	Fe	K	Mg	Mn	Ni	Pb	Zn
Wastewater effluent *before* adsorption	79 ± 3	1 ± 0.03	439 ± 38	268 ± 6	18,318 ± 358	1,977 ± 20	243 ± 6	184 ± 5	2,000 ± 107	6 ± 0.2	26 ± 1
Wastewater effluent *after* adsorption	57 ± 2	0.39 ± 0.04	405 ± 5	282 ± 5	9,655 ± 262	58 ± 2	4.68 ± 0.23	151 ± 4	1,829 ± 8	1 ± 0.13	17 ± 0.38

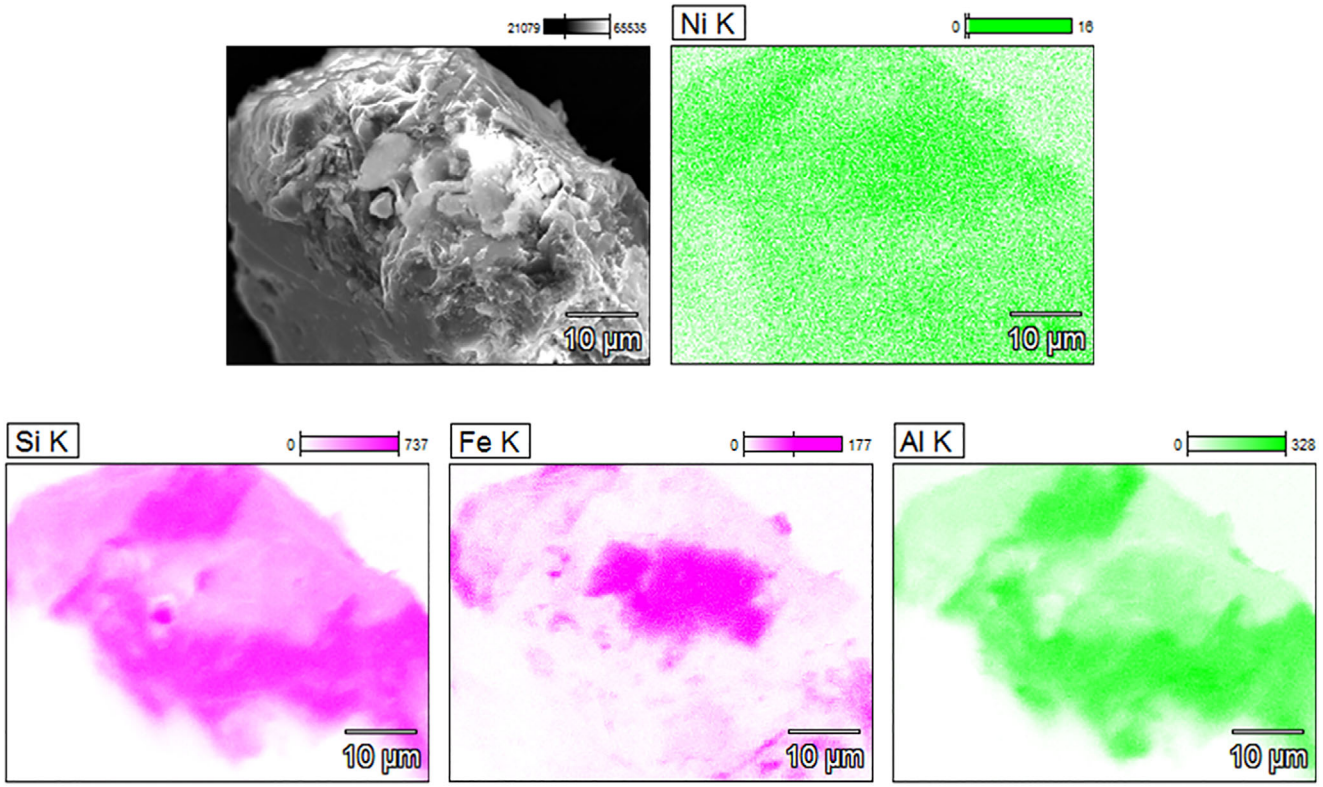

FIGURE 4 | EDS elemental map for the zeolitic concentrate after the adsorption procedure.

of simultaneously interacting with different cations. The removal of Fe^{3+} (from 18 318 to 9655 mg L^{-1}), K^{+} (from 1977 to 58), and Ca^{2+} (from 79 to 57 mg L^{-1}), in particular, demonstrates that these ions also participate actively in ion exchange processes, competing for the same active sites as Ni^{2+}. This competitive adsorption behavior is characteristic of zeolitic materials with negatively charged surfaces, where ions with higher charge densities and smaller hydration radius, such as Pb^{2+} and Fe^{3+}, tend to occupy energetically more favorable positions within the zeolitic framework [27, 28].

The EDS mapping analysis (Figure 4) corroborates these findings, revealing the presence of Ni and Fe signals distributed over the zeolite surface after adsorption, alongside the characteristic Si and Al elements from the sodalite structure. The homogeneous dispersion of Ni throughout the analyzed region indicates that the adsorption process occurred not only on the external surface but also within accessible mesopores, consistent with ion-exchange mechanisms. The detection of Fe, in turn, suggests partial retention of this ion from the effluent, supporting the hypothesis of competitive adsorption among multivalent cations. The coexistence of Si and Al signals confirms the structural integrity of the sodalite framework after interaction with the effluent, indicating that the ion-exchange process did not compromise the material's crystalline matrix.

The observed reduction in Cd^{2+} (from 1.0 to 0.39 mg L^{-1}) and Pb^{2+} (from 6.0 to 1.0 mg L^{-1}) also supports the occurrence of multi-ion adsorption, confirming that the synthesized sodalite can simultaneously remove trace contaminants even under high ionic strength conditions. The slight variations in Mn^{2+} and Zn^{2+} concentrations after the adsorption process may be attributed to secondary adsorption mechanisms, such as electrostatic attraction and surface complexation, which complement the predominant ion-exchange process. These results highlight that, despite the strong competition among coexisting cations, the synthesized zeolitic concentrate maintains significant adsorption capacity for Ni^{2+} and other contaminant elements.

Therefore, the material's performance in real wastewater demonstrates its robustness and applicability under complex environmental conditions, where multiple ions coexist and compete for the same active sites. This characteristic makes the zeolitic concentrate derived from alum sludge a promising, low-cost, and sustainable adsorbent for integrated wastewater treatment, contributing not only to the selective removal of priority contaminants such as Ni^{2+} but also to the overall reduction of metal load in effluents. It is worth highlighting that desorption and regeneration assays were not investigated in the present study, as the primary focus was to assess the adsorbent performance under realistic conditions involving complex ionic competition. Nevertheless, regeneration efficiency and multi-cycle stability are recognized as important aspects for practical implementation. Moreover, in this study, adsorption experiments were designed to determine the maximum adsorption capacity of the zeolitic concentrate and to comparatively evaluate its affinity toward different metal ions under equilibrium conditions. Although adsorption isotherm models, such as Langmuir and Freundlich, are widely used for thermodynamic interpretation, their application is more appropriate for simplified single-ion systems. The high concentration range investigated and the presence of competitive ions in real wastewater limit the direct applicability of classical isotherm parameters.

4 | Conclusion

Sodalite from alum sludge using an autoclave and hydrothermal treatment proved to be an effective and scalable strategy for producing zeolitic materials with potential environmental applications. The zeolitic concentrate exhibited characteristic sodalite phases, a mesoporous morphology, and a negative surface charge, which favors the adsorption of cationic metals. The material showed great adsorption capacities for Pb^{2+} (189 mg g^{-1}), Cd^{2+} (121 mg g^{-1}), and Ni^{2+} (58.4 mg g^{-1}), while exhibiting low affinity for Cr^{6+}, due to charge repulsion effects. In real wastewater, the adsorption performance decreased due to competitive interactions with coexisting ions, yet the material maintained a relevant removal efficiency for Ni^{2+}. These findings demonstrate that sodalite derived from alum sludge is a promising low-cost adsorbent for wastewater treatment, simultaneously contributing to waste valorization and the circular economy. Further studies are needed to elucidate the mechanisms that control the adsorption rate, as well as to address detailed kinetic modeling.

Author Contributions

Raquel Cardoso Machado: Conceptualization, Methodology, Formal analysis, Investigation, Writing – original draft, Writing – review & editing, Visualization and Project administration; Vinicius Ferraz Majaron: Conceptualization, Methodology, Formal analysis, Investigation, Writing – review & editing and Visualization; Alexandre Antonio Fidelis Martins Junior: Methodology and Visualization; Nathália Liz Barriosa: Methodology, Formal analysis, Investigation and Visualization; Welton de Araujo Cintra Junior: Visualization. Ricardo Bortoletto-Santos: Conceptualization, Methodology, Formal analysis, Investigation, Writing – original draft, Writing – review & editing, Visualization, Supervision. Caue Ribeiro: Writing – original draft, Writing – review & editing, Visualization, Supervision, Resources, Project administration, Funding acquisition.

Acknowledgements

The Article Processing Charge for the publication of this research was funded by the Coordenacao de Aperfeicoamento de Pessoal de Nivel Superior - Brasil (CAPES) (ROR identifier: 00x0ma614).

Funding

The authors thank FAPESP (São Paulo State Research Foundation, project number 2020/12210-3, 2023/01549-8, 2025/22529-0 and grant 2022/09773-1), FINEP (MATFERT 01.22.0274.00, FertBrasil 01.22.0080.00 Ref. 1219/21 and 01.24.0554.00), CAPES, and National Council for Scientific and Technological Development (CNPq, grants 402713/2023-0 and 408961/2025-2, CNPq INCT Circularidade 406925/2022-4), for the financial support. The authors are grateful for the institutional support provided by the Basic Sanitation Company of the State of São Paulo (SABESP) and the support facilities offered by the Agronano Network (Embrapa Research Network), the National Nanotechnology Laboratory for Agribusiness (LNNA), and the Laboratory of Process and Materials (ProMat—UNAERP).

Conflicts of Interest

The authors declare no conflicts of interest.

Data Availability Statement

Datasets of this study will be made available from the corresponding author on request.

References

1. WWAP (United Nations World Water Assessment Programme), *The United Nations World Water Development Report 2017: Wastewater—The Untapped Resource* (2017), https://unesdoc.unesco.org/ark:/48223/pf0000247153.

2. P. Borah, M. Kumar, and P. Devi, "Types of Inorganic Pollutants: Metals/Metalloids, Acids, and Organic Forms," *Inorganic Pollutants in Water* (Elsevier, 2020), 17–31, https://doi.org/10.1016/B978-0-12-818965-8.00002-0.

3. E. P. Ferreira-Neto, S. Ullah, T. C. A. da Silva, et al., "Bacterial Nanocellulose/MoS_2 Hybrid Aerogels as Bifunctional Adsorbent/Photocatalyst Membranes for in-Flow Water Decontamination," *ACS Applied Materials & Interfaces* 12 (2020): 41627–41643, https://doi.org/10.1021/acsami.0c14137.

4. M. Jaishankar, T. Tseten, N. Anbalagan, B. B. Mathew, and K. N. Beeregowda, "Toxicity, Mechanism and Health Effects of some Heavy Metals," *Interdisciplinary Toxicology* 7, no. 2 (2014): 60–72, https://doi.org/10.2478/intox-2014-0009.

5. S. Mitra, A. J. Chakraborty, A. M. Tareq, et al., "Corrigendum to 'Impact of Heavy Metals on the Environment and Human Health: Novel Therapeutic Insights to Counter the Toxicity'," *Journal of King Saud University—Science* 35, no. 7 (2023): 102823, https://doi.org/10.1016/j.jksus.2023.102823.

6. K. Jomova, S. Y. Alomar, E. Nepovimova, K. Kuca, and M. Valko, "Heavy Metals: Toxicity and Human Health Effects," *Archives of Toxicology* 99 (2025): 153–209, https://doi.org/10.1007/s00204-024-03903-2.

7. Z. Sun, Y. Liao, Y. Zhang, et al., "Sustainable Carbon Materials in Environmental and Energy Applications," *Sustainable Carbon Materials* 1 (2025): 007, https://doi.org/10.48130/scm-0025-0002.

8. X. Pan, J. Jiahui N. Zhang, and M. Xing, "Research Progress of Graphene-Based Nanomaterials for the Environmental Remediation," *Chinese Chemical Letters* 31 (2020): 1462–1473, https://doi.org/10.1016/j.cclet.2019.10.002.

9. M. Xiao, X. Zhang, X. Liu, Z. Chen, X. Tai, and X. Wang, "Recent Progress in Covalent Organic Framework-Based Membranes: Design, Synthesis, and Applications in the Fields of Energy and the Environment," *ACS Macro Letters* 14 (2025): 1201–1220, https://doi.org/10.1021/acsmacrolett.5c00403.

10. L. Marchiori, M. V. Morais, A. Albuquerque, L. Andrade Pais, and V. Cavaleiro "Testing Methodologies to Evaluate Waste-Based Liners," in *Geotechnical Engineering Challenges to Meet Current and Emerging Needs of Society* (CRC Press, 2024), 3129–3132, https://doi.org/10.1201/9781003431749.

11. M. E. Borges, T. Hernández, and P. Esparza, "Photocatalysis as a Potential Tertiary Treatment of Urban Wastewater: New Photocatalytic Materials," *Clean Technologies and Environmental Policy* 16 (2014): 431–436, https://doi.org/10.1007/s10098-013-0622-9.

12. United Nations, 2015, Transforming Our World: The 2030 Agenda for Sustainable Development, https://www.un.org/sustainabledevelopment/.

13. H. Shen, R. Zou, Y. Zhou, et al., "Additive Manufacturing of Sodalite Monolith for Continuous Heavy Metal Removal From Water Sources," *Chinese Journal of Chemical Engineering* 42 (2022): 82–90, https://doi.org/10.1016/j.cjche.2021.12.016.

14. R. C. Machado, S. F. Valle, I. R. S. Chao, and C. Ribeiro, "Valorization of Alum Sludge Waste through Zeolite Synthesis for Sustainable Fertilizer Production," *Materials Research* 27 (2024): 20240269, https://doi.org/10.1590/1980-5373-MR-2024-0269.

15. M. Arockiaraj, J. Clement, D. Paul, and K. Balasubramanian, "Quantitative Structural Descriptors of Sodalite Materials," *Journal of Molecular Structure* 1223 (2021): 128766, https://doi.org/10.1016/j.molstruc.2020.128766.

16. N. V. Chukanov and S. M. Aksenov, "Structural Features, Chemical Diversity, and Physical Properties of Microporous Sodalite-Type Materials: A Review," *International Journal of Molecular Sciences* 25, no. 18 (2024): 10218, https://doi.org/10.3390/ijms251810218.

17. S. Lin, X. Jiang, Y. Zhao, and J. Yan, "Zeolite Greenly Synthesized From Fly Ash and Its Resource Utilization: A Review," *Science of The Total Environment* 851 (2022): 158182, https://doi.org/10.1016/j.scitotenv.2022.158182.

18. A. Grela, K. Kuc, and T. Bajda, "Application of Zeolites and Mesoporous Silica Materials for Removal of NSAIDs and Antibiotics From Water: A Review," *Materials* 14 (2021): 4994, https://doi.org/10.3390/ma14174994.

19. M. Esaifan, L. N. Warr, G. Grathoff, et al., "Synthesis of Hydroxy-Sodalite/Cancrinite Zeolites From Calcite-Bearing Kaolin for the Removal of Heavy Metal Ions in Aqueous Media," *Minerals* 9, no. 8 (2019): 484, https://doi.org/10.3390/min9080484.

20. B. Hrovat, "Industrial Waste Management: Fly Ash Zeolites and Microplastics," (PhD diss., University of Eastern Finland, 2024), http://urn.fi/URN:ISBN:978-952-61-5451-0.

21. M. Karhu, J. Lagerbom, S. Solismaa, et al., "Mining Tailings as Raw Materials for Reaction-Sintered Aluminosilicate Ceramics: Effect of Mineralogical Composition on Microstructure and Properties," *Ceramics International* 45, no. 4 (2019): 4840–4848, https://doi.org/10.1016/j.ceramint.2018.11.180.

22. M. Ritter, H. Schilling, H. Brüggemann, et al., "Towards Achieving the Sustainable Development Goals: A Collaborative Action Plan Leveraging the Circular Economy Potentials," *Gruppe Interaktion Organisation Zeitschrift für Angewandte Organisationspsychologie (GIO)* 55 (2024): 175–187, https://doi.org/10.1007/s11612-024-00765-4.

23. J. Li, X. Zeng, X. Yang, C. Wang, and X. Luo, "Synthesis of Pure Sodalite With Wool Ball Morphology From Alkali Fusion Kaolin," *Materials Letters* 161 (2015): 157–159, https://doi.org/10.1016/j.matlet.2015.08.058.

24. S. Zeng, R. Wang, Z. Zhang, and S. Qiu, "Solventless Green Synthesis of Sodalite Zeolite Using Diatomite as Silica Source by a Microwave Heating Technique," *Inorganic Chemistry Communications* 70 (2016): 168–171, https://doi.org/10.1016/j.inoche.2016.06.013.

25. S. Golbad, P. Khoshnoud, and N. Abu-Zahra, "Hydrothermal Synthesis of Hydroxy Sodalite From Fly Ash for the Removal of Lead Ions From Water," *International Journal of Environmental Science and Technology* 14 (2017): 135–142, https://doi.org/10.1007/s13762-016-1133-x.

26. M. Yoldi, E. G. Fuentes-Ordoñez, S. A. Korili, and A. Gil, "Zeolite Synthesis From Aluminum Saline Slag Waste," *Powder Technology* 366 (2020): 175–184, https://doi.org/10.1016/j.powtec.2020.02.069.

27. L. Velarde, M. S. Nabavi, E. Escalera, M.-L. Antti, and F. Akhtar, "Adsorption of Heavy Metals on Natural Zeolites: A Review," *Chemosphere* 328 (2023): 138508, https://doi.org/10.1016/j.chemosphere.2023.138508.

28. Y. Dehmani, B. B. Mohammed, R. Oukhrib, et al., "Adsorption of Various Inorganic and Organic Pollutants by Natural and Synthetic Zeolites: A Critical Review," *Arabian Journal of Chemistry* 17, no. 1 (2024): 105474, https://doi.org/10.1016/j.arabjc.2023.105474.

29. H. Pahlavanzadeh and M. Motamedi, "Adsorption of Nickel, Ni(II), in Aqueous Solution by Modified Zeolite as a Cation-Exchange Adsorbent," *Journal of Chemical & Engineering Data* 65, no. 1 (2020): 185–197, https://doi.org/10.1021/acs.jced.9b00868.

30. W. Liu, T. Wang, A. G. L. Borthwick, et al., "Adsorption of Pb^{2+}, Cd^{2+}, Cu^{2+} and Cr^{3+} Onto Titanate Nanotubes: Competition and Effect of Inorganic Ions," *Science of The Total Environment* 456-457 (2013): 171–180, https://doi.org/10.1016/j.scitotenv.2013.03.082.